ANNALS OF GEOPHYSICS, 68, 2, A214, 2025; doi:10.4401/ag-9161
OPEN ACCESS

The impact of Mother's Day Storms in May 2024 on Precise Point Positioning at mid-latitudes

Jihye Park[*,1], Luca Spogli[2], Althaf Azeez[1], Lucilla Alfonsi[2], Claudio Cesaroni[2], Vincenzo Romano[2], Adedayo Akande[1]

(1) Oregon State University, Corvallis, USA
(2) Istituto Nazionale di Geofisica e Vulcanologia, Rome, Italy

Article history: received September 25, 2024; accepted January 25, 2025

Abstract

Geomagnetic storms generate disturbances in the ionosphere that can significantly affect the quality of Global Navigation Satellite System (GNSS) signals transmitted through the ionosphere. While many studies have investigated their impact on GNSS at low or high latitudes as they are the regions mostly affected by ionospheric disturbances, this study focuses on the mid-latitude area affected by a recent superstorm event in May 2024, namely Mother's Day storm. Due to the severity of the Mother's Day storm, the visible blueprint of the ionospheric irregularities – aurorae and stable auroral arcs – were observed at mid-latitudes worldwide, thus motivating our research. By probing the GNSS measurements recorded at a GNSS receiver, the ionospheric variations and their impact on the GNSS positioning can be evaluated. We processed GNSS data recorded at Lampedusa Island in Italy during the Mother's Day storm and analyzed the variation of the total electron content (TEC), scintillation indices, and the accuracy of precise point positioning (PPP) results. During the storm, the TEC dramatically decreased, which suggests no significant impact on positioning since TEC is positively correlated with the ionospheric code delay and phase advance in the GNSS signals. However, the PPP results indicate that the geomagnetic storm degraded the GNSS positioning considerably due to the scintillation occurrence during the storm event.

Keywords: GNSS Positioning; Mother's Day Storms; Ionospheric disturbances; Precise Point Positioning

1. Introduction

As of the year 2024, the sunspot numbers are increasing close to the solar maximum in the 25th solar cycle. Several interplanetary coronal mass ejections (ICMEs) reached the Earth's magnetosphere on 10 May 2024 causing the strongest geomagnetic storm since November 2003. During the May 2024 storm, named hereafter as "Mother's Day storm", the Kp index on 10-11 May 2024 reached up to 9, and Dst index reached down to –412 nT. Between 10 and 13 May 2024, *aurorae* and stable auroral arcs were seen across the United States as far south as Florida, Europe as far south as Spain, Africa-Algeria and the Canary Islands, and Asia including China, Japan, and India. Spogli et al. (2024) reported the space weather effects in the Mediterranean region, where a dense network of GNSS receivers (including

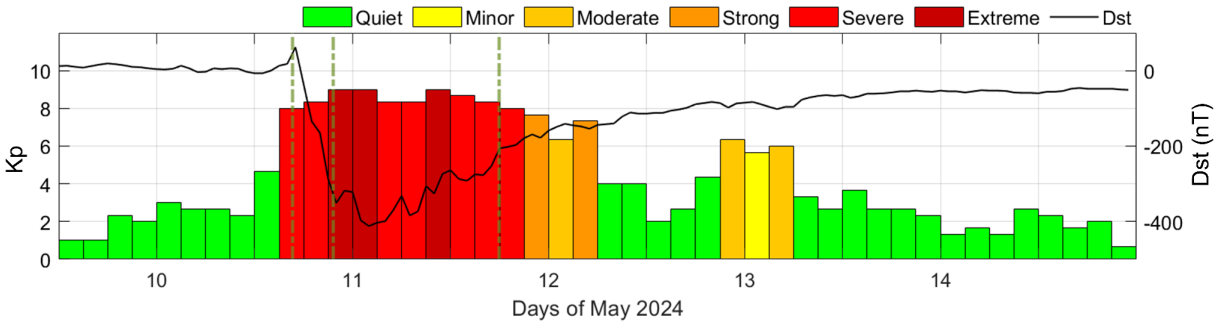

Figure 1. Kp index and Dst index, with the color code in the panel representing the NOAA Space Weather Scale for geomagnetic storms (NOAA Space Weather Scales). The green dashed lines mark the arrival of the interplanetary shocks. The data covers the period from May 9, 2024, 12:00 UT to May 14, 2024, 23:59 UT.

scintillation receivers) and ionosondes recorded significant modifications induced by the storm on the ionosphere. Among other results, the authors presented a significant decrease in plasma density on 11 May, visible as an intense negative (decrease of about 70%) and long-lasting (two days) ionospheric storm visible on the critical frequency of the ionospheric F2 layer (foF2) and TEC over Italy. These observations indicate the severeness of the space weather effects on that day. Themens et al. (2024) and Evans et al. (2024) observed ionospheric disturbances at high latitudes and discussed the transportation of them toward the mid/low latitudes which indirectly discuss the 2024 May storm events' impact on the mid latitudes. Guo et al. (2024) presented a comprehensive study of the F-region ionospheric storm effect mainly at mid and low latitude of East Asian area during the May 2024 super geomagnetic storm based on multiple datasets and analyzed the positive and negative storm effects on each dataset. These findings well demonstrate the impact of the storm events in the upper and lower atmospheres observed at high, mid, and low latitudes.

Increased solar activities significantly influence satellite operations and GNSS signals. Luo et al. (2018) assessed the performance of GPS precise point positioning (PPP) under the various levels of geomagnetic storms during solar cycle 24. They processed 500 International GNSS Service (IGS) stations around the world and analyzed the statistics of the PPP solutions of stations at low-, mid-, and high-latitudes, respectively. The result showed that the PPP performance at high latitudes was significantly degraded due to the geomagnetic storm events while the mid and low latitudes were not directly affected by the storm intensity. This result is reasonable because the high latitude region is featured by a strong coupling among the interplanetary medium, the magnetosphere, the thermosphere, and the ionosphere (Nava et al., 2016; Luo et al., 2018). In fact, on one hand, the presence of medium-to-small-scale irregularities (kilometers to hundreds of meters scales) causes refractive and diffractive (only small-scale, i.e. hundreds of meters scales) effects on the signals (Wernik et al., 2003), increasing the probability loss of lock events, cycle slips, and degradation of the accuracy of GNSS-based positioning (Vadakke Veettil and Aquino, 2021). On the other hand, the principal source of irregularities at low latitudes is represented by the post-sunset Equatorial Plasma Bubbles (EPBs). They occur almost daily under high solar flux and equinoctial conditions (Li et al., 2021; Perez-Macho et al., 2022; Pica et al., 2024), while solstitial conditions results into longitudinal dependence and pre-/post-midnight dependence of the EPBs occurrence (see, e.g. Yizengaw and Groves, 2018; Aa et al., 2020). The occurrence of Equatorial Plasma Bubbles is modulated by various factors, including geomagnetic storms, which can influence the geographical location and characteristics of the scintillation phenomenon.

Basu et al. (2008) analyzed the GPS phase fluctuations, regional TEC maps, *in situ* measurements of sub-auroral polarization streams (SAPS), and auroral convection measurements during the intense geomagnetic storm on 7-8 November 2004. Their findings stated the possible impact of the large ionospheric velocities on GPS-based navigation systems. However, the study did not include the actual GNSS positioning errors at mid-latitudes. Shinbori et al. (2021) investigated the statistical behavior of ionospheric disturbances from high- to mid-latitudes during geomagnetic storms from 2000 to 2019. The authors indicated the different types of responses at mid- and high latitudes, respectively, to the same storms. Kashcheyev et al. (2018) also found that the same storm produced different effects (positive or negative) depending on the longitudinal sector during the May 2015 storm.

As revealed in the literature, the effect of different historical geomagnetic storms in the ionosphere varied in different regions. A geomagnetic storm leads positive or negative impact on TEC in the ionosphere (Mendillo, 2006; Basu et al., 2008) and consequently drives different types of disturbances in the ionosphere (Shinbori et al., 2021). It degrades the performance of GNSS positioning at a certain location while the other regions are not affected

(Luo et al., 2018). Because of the unpredictable variations and disturbances of TEC depending on events in the past and the complexity of the ionospheric coupling with the geo-space, thermosphere and the lower atmospheric layers, the consequences of a geomagnetic storm may not be predicted.

In this study, we explored the impact of the strongest geomagnetic storm in solar cycle 25 to a mid-latitude region in which the effect of a geomagnetic storm is considered to be weaker than in other regions. To analyze the ionospheric responses to the severe geomagnetic storms in May 2024, we examined the temporal variations of TEC and the scintillation occurrence during the period of Mother's Day storm (9-15 May 2024), then evaluated their influence on GNSS positioning by checking PPP results during the same period as well as the five most quiet and five disturbed days in May 2024.

This study is unique in its focus on GNSS performance degradation at mid-latitude regions, where GNSS-impacting ionospheric irregularities are generally less frequent compared to equatorial and high-latitude zones. By evaluating the spill-over effects of equatorial plasma bubbles (EPBs) during the Mother's Day storm, this research provides new insights into the mechanisms that extend ionospheric disturbances to typically less-affected areas. Such findings fill a critical gap in the current understanding of GNSS vulnerability under extreme space weather conditions in an area, the Mediterranean, in which GNSS applications cover critical services.

Section 2 presents the TEC and scintillation indices during the Mother's Day storm measured by a ground based GNSS receiver at mid-latitude, specifically Lampedusa in Italy. The TEC variations and the scintillation occurrence can demonstrate the ionospheric responses to the geomagnetic storm. In Section 3, we evaluated the impact of the storm on GNSS observations by assessing the GNSS positioning performance during the storm event. Section 4 summarizes the outcome, and Section 5 concludes the research findings.

2. Ionospheric responses at Lampedusa, Italy

The Istituto Nazionale di Geofisica e Vulcanologia (INGV in Italy) manages an Ionospheric Scintillation Monitor Receiver (ISMR, station ID: LAM0P) in Lampedusa Island. The geodetic coordinates of LAM0P are 35.52°N, 12.63°E (geomagnetic latitude from IGRF-13 in 2024 is 35.75N) and the site is equipped with a Septentrio PolaRx5s receiver and a choke ring antenna. PolaRx5s is a multi-frequency, multi-constellation GNSS receiver equipped with low-noise OCXO oscillators (Bougard et al., 2011). It measures raw phase and post-correlation in-phase (I) and quadrature (Q) components at a configurable sampling rate between 50 and 100 Hz. Its firmware is capable of providing phase and amplitude scintillation indices S4 and (Yeh and Liu, 1982; Wernik et al., 2003) at a 1-minute cadence for every satellite in view and for every available frequency. In this paper, we rely on the S4 and indices calculated from the L1-C/A (GPS and GLONASS), E1/L1BC (Galileo), and B1 (BeiDou) 50 Hz raw signal samples. The ISMR in Lampedusa has been proven to be very effective in detecting GNSS scintillation (Spogli et al., 2024; Pica et al., 2024), impacting positioning accuracy due to the presence of ionospheric irregularities (Park et al., 2017), and to the presence of artificial radio frequency interference (Pica et al., 2023).

Being a dual frequency receiver, it can effectively estimate the TEC by using the calibration technique introduced by Ciraolo et al. (2007) that has been widely used in many applications related both to ionospheric studies (Cesaroni et al., 2017; Alfonsi et al., 2021; Spogli et al., 2023, 2021) and space weather service and tools (Cesaroni et al., 2021; Tornatore et al., 2021; Kauristie et al., 2021; Pignalberi et al., 2024). The ionospheric behaviors during the Mother's Day storm in Lampedusa were observed by analyzing GNSS data recorded at LAM0P and the ionospheric responses to the storm were presented in this section.

2.1 Ionospheric Scintillations

Figure 2 shows the time series of S4 (a) and (b) of the first frequency, i.e., GPS L1, GLONASS G1, Galileo E1, and BeiDou B1, emitted from all satellites in view above 30° elevation as seen by the ISMR in Lampedusa. Different colors correspond to different Space Vehicle IDs (SVIDs), described in Table 1, which relates the SVID range, their GNSS constellation and Pseudorandom Noise (PRN) numbers, and Receiver Independent Exchange Format (RINEX) satellite codes.

As already highlighted by Spogli et al. (2024), the Mother's Day storm triggered the spill-over of small-scale ionospheric irregularities embedded in the EPBs from lower latitudes, entering the field of view of the GNSS

SVID	Description	RINEX satellite code
1-37	PRN number of GPS satellites	Gnn (nn = SVID)
38-61	Slot number of GLONASS satellites with the offset of 37 (R01 to R24)	Rnn (nn = SVID-37)
63-68	Slot number of GLONASS satellites with the offset of 38 (R25 to R30)	Rnn (nn = SVID-38)
71-106	PRN number of GALILEO satellites with the offset of 70	Enn (nn = SVID-70)
141-177	PRN number of BeiDou satellites with the offset of 140	Cnn (nn = SVID-140)

Table 1. Satellite Vehicle IDs (SVID), PRNs and RINEX satellites codes.

receivers, as proved by increases of S4 and in the considered range of elevation angles and starting around 19:00 UTC on 10 May. Specifically, their Fig. 9 clearly shows that, during the night of May 10-11, the storm's arrival induces undershielding conditions, altering the Region 1 and Region 2 Field-Aligned Currents (FACs) and triggering Prompt Penetration Electric Fields (PPEFs) at local sunset near the magnetic equator in the studied longitudinal sector. This is reflected in the increase of the variation in the equatorial electric field (EEF) during the Pre-Reversal Enhancement (PRE) at sunset, leading to a stronger EB drift at the magnetic equator and a consequent uplift of the F region. This mechanism allows EPBs to enter the field of view of the Lampedusa GNSS.

As shown in Fig. 2, signals from the multiple satellite vehicles of all four constellations were affected by the scintillations that led to the high peaks in S4 and about the same epochs around the end of DOY 131 (10 May 2024) that was the period of Dst dramatically dropped and the severity of the geomagnetic storm significantly increased based on the Kp index as indicated in Fig. 1. The spill-over was caused by the increased uplift of the F-layer triggered by the occurrence of Prompt Penetrating Electric Fields (PPEFs) at the storm's arrival on the magnetosphere, i.e. around 16:40 UT on 10 May. The recovery phase of the storm is featured by conditions of the Equatorial

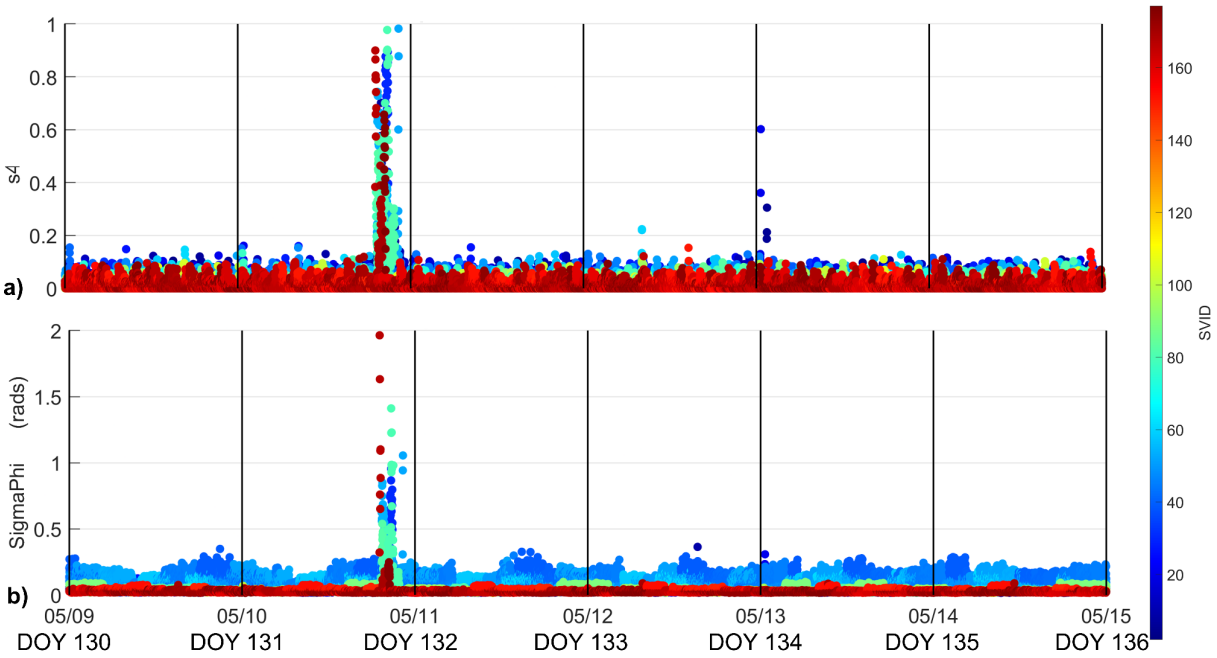

Figure 2. Time series of S4 (a) and (b) evaluated for the first frequency emitted from all satellites in view above 30° elevation as seen by the ISMR in Lampedusa. Different colors correspond to different SVIDs.

Electrojet (EEJ) and of the Pre-reversal Enhancement (PRE) which do not result in further spill-over at high elevation angles of irregularities in the field of view of the ISMR in Lampedusa. This is likely due to the effect of disturbance dynamo electric fields (DDEFs) (Yamazaki and Maute, 2017), which are driven by enhanced Joule heating and neutral wind dynamics and a have delayed effects (1-3 hours) lasting up to 1-2 days after geomagnetic activity subsides (Spogli et al., 2016; Alfonsi et al., 2011, 2021; Tulasi Ram et al., 2016).

2.2 Total Electron Content

To understand the background ionospheric conditions under which the EPB spill-over takes place, this section presents the TEC variations around the storm period. Figure 3 shows the vertical TEC (vTEC) time series plots around the period of the Mother's Day storm, i.e., 9-15 May 2024. The time series shown in black is the actual vTEC values calculated every 10 minutes. The red dashed line in Fig. 3 indicates the vTEC quiet reference, evaluated as the median values during the 27 days preceding the storm occurrence.

The notable decrease of TEC in Fig. 3 is triggered by the severe depletion of the [O]/[N2] ratio induced by the disturbed thermospheric circulation related to the severe geomagnetic storm events (Spogli et al., 2024).

TEC values were significantly lower than the reference TEC (i.e. the red dashed line) during almost the entire period of this storm on May 11th, featuring this event as a negative storm in the area of Lampedusa, Italy, as also shown in (Spogli et al., 2024). A second increase of Kp occurred on the 12th of May (Kp index was 6^{+} at 21:00 UTC) and lasted until early on the 13th of May (Kp index was 6 at 3:00 UTC). Corresponding to this event, amplitude scintillations were observed around 0:00 UTC on May 13th, coinciding with a depleted ionosphere, as evidenced by the negative TEC storm signatures recorded until the end of that day. This second scintillation event can be again linked to the spill-over of EPBs likely triggered by disturbances in the EEF linked to the second Kp increase (see Fig. 9 of Spogli et al., 2024).

While both types of ionospheric measurements from GNSS presented the severe geomagnetic storm effect, each type of observed quantities responded differently. The scintillations occurred during a short period of time that is immediately after the storm activated whereas the TEC remained decreased during the presence of the storm events. In the following section, we analyze the impact of the interplay between the EPB spill-over and the negative TEC storm on GNSS positioning performance by evaluating several different elements of GNSS signal processing.

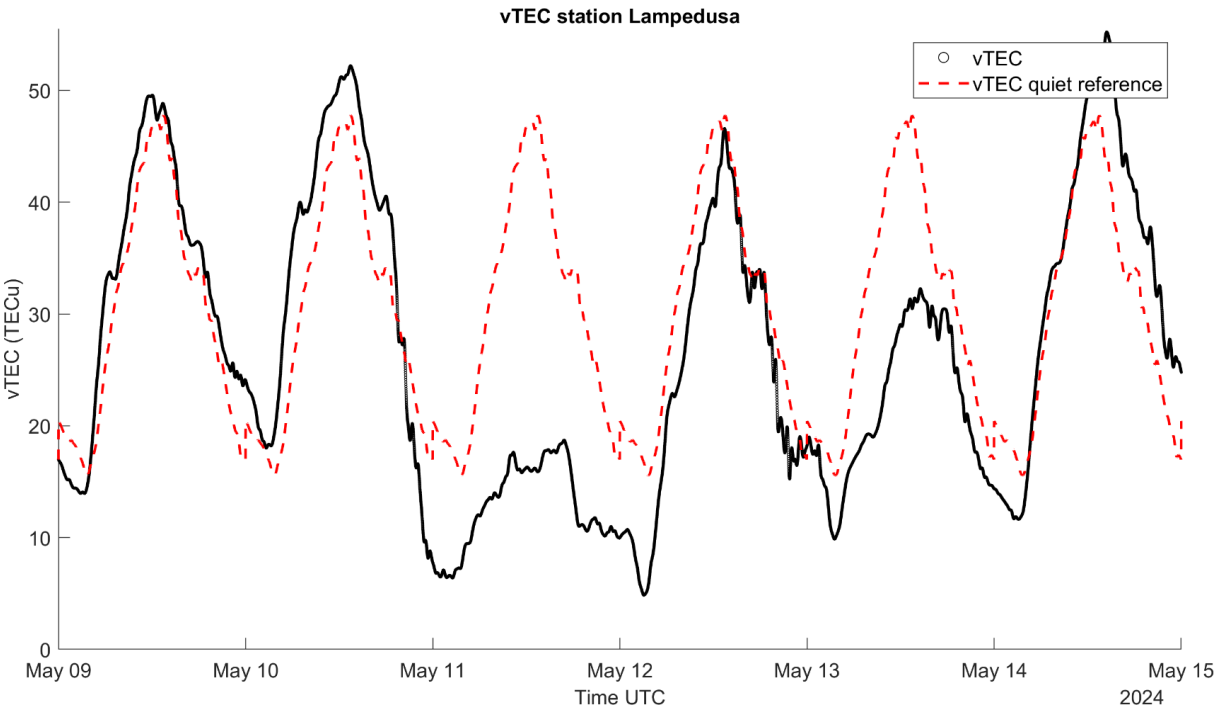

Figure 3. vTEC variations observed at Lampedusa, Italy. The black solid line represents the actual values, while the red dashed line represents the quiet values, used as reference.

3. GNSS Positioning Performance during Geomagnetic Storms

As there are highly densified GNSS networks worldwide, GNSS observations can serve as a great tool for monitoring the effect of space weather in the ionosphere anywhere around the world. For the space weather community, a dense GNSS network plays an important role in continuously observing the electron content in the ionosphere.

At the same time, the impact of extreme space weather events is a significant degradation of the GNSS positioning performance (Aquino et al., 2009; Park et al., 2017). The degradation of GNSS performance is a critical problem especially when it is associated with safety. For example, the International Civil Aviation Organization is aware of the impact of space weather events on civil aviation and puts effort into mitigating the risk by generating advisories for pilots supporting the civil aviation communities (Kauristie et al., 2021). Although the mid-latitude regions are known as being less affected by global-scale geomagnetic storms in terms of GNSS positioning, different responses can be expected as addressed by literature (e.g. Rodrigues et al., 2021; Mrak et al., 2024).

As shown in Section 2, the Mother's Day superstorm featured strong and long-lasting negative storm conditions in the considered sector, as the TEC decreased rapidly in response to the storm events during 10-11 May 2024. While smaller TEC values are to cause smaller delays in GNSS signals of GNSS signals, other effects such as ionospheric scintillations can affect the performance of GNSS positioning.

Figure 4 shows the second order time difference of the ionospheric delay, referred to as SDTD-iono on GPS (a), Galileo (b), and GLONASS (c). The SDTD-iono is the quantity showing the temporal dynamics of the ionospheric delay on the line of sight after removing the major trend of the ionospheric delay time series that is highly affected by the geometry changes between the satellite and the receiver on the ground and the solar diurnal effect. The SDTD-iono time series are plotted over the Dst values. (d) shows the amplitude scintillation index, S4, which allows observing

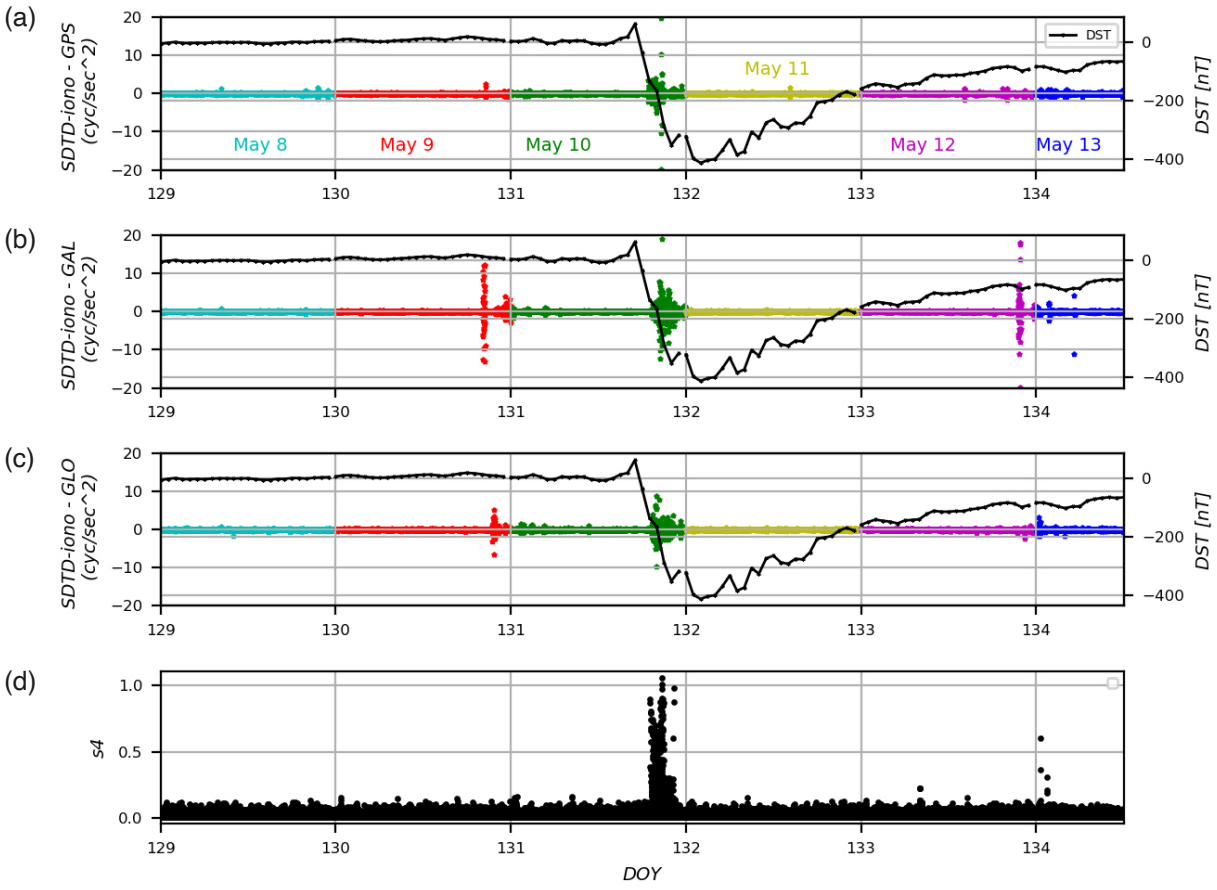

Figure 4. The second order time difference of the ionospheric delay (SDTD-iono) showing the temporal dynamics of the ionospheric delay from DOY 129 to DOY 134 recorded at Lampedusa, Italy (Station ID: lam0p, 35.52°N, 12.63°E). (a), (b) and (c) present the SDTD-iono of GPS, Galileo, and GLONASS signals, respectively, and corresponding Dst values are also shown in black. (d) shows the S4 indices during the corresponding period.

the SDTD-iono and the scintillation occurrence over time. It is seen that there is a significant drop in the Dst value on the most disturbed day, DOY 131 in green, and the SDTD-iono also significantly increased at the same time as shown in the figure for all three constellations. During that time, strong scintillations occurred as S4 reached over 1.0. It can be interpreted that the Dst variation and scintillations affected the temporal variation of the ionospheric delay. As already shown in the previous section, this occurs in correspondence with the spill-over EPBs in the ISMR field of view, and it may cause the degradation of GNSS positioning capability that is shown in this section.

Spogli et al. (2024) presented a significant enhancement of the rate of TEC change index (ROTI) based on 5 minutes observations on 10-11 May 2024. This ROTI enhancement testifies the presence of medium scale irregularities (Spogli et al., 2023). In Fig. 4, the Dst significantly dropped at the end of May 10th where the high disturbances of the SDTD-iono occurred during the same period. It should be noted that there are high peaks at the end of May 9th (DOY 130, indicated in red) when the Kp index started increasing, but its impact varies depending on constellations. While the GPS constellations were less affected by the ionospheric disturbances, GLONASS and Galileo showed high peaks.

To better investigate the impact of the geomagnetic storms during the selected days, we analyze the GNSS positioning performance before, and during the geomagnetic storms by processing PPP in kinematic mode using the CSRS-PPP tool (https://webapp.csrs-scrs.nrcan-rncan.gc.ca/geod/tools-outils/ppp.php). It should be noted that we adopted the kinematic mode data processing to effectively assess the impact of the geomagnetic storm on the positioning performance during the storm period rather than evaluating the static positioning result. It should be noted that the CSRS-PPP tool only used GPS and GLONASS, so the positioning results in this section are the data processing results from GPS and GLONASS observations.

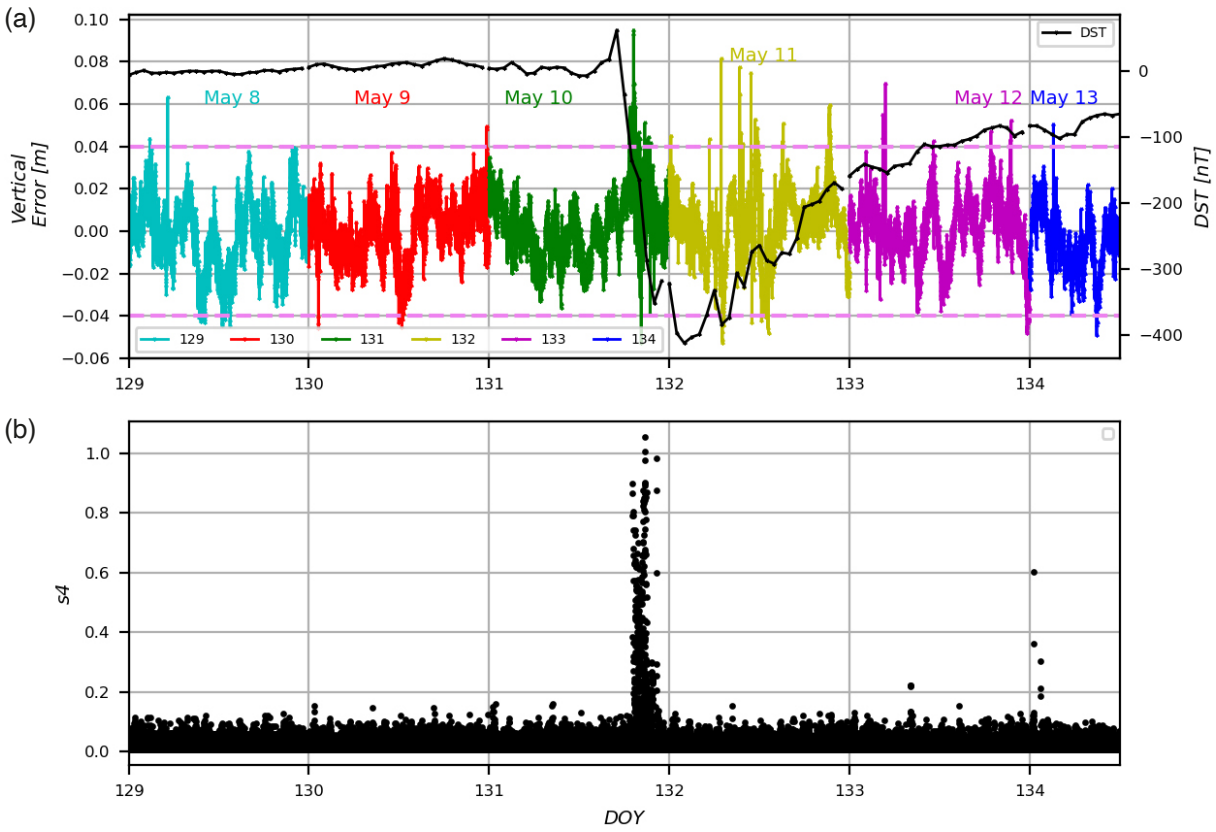

Figure 5. The kinematic PPP vertical error with the Dst (a) and Kp indices (b) from DOY 129 to DOY 134.

Figure 5 shows the kinematic PPP vertical error with the Dst (a) and Kp indices (b) from DOY 129 to DOY 134. On DOY 131 and DOY 132, the vertical error of the PPP solution reached up to 8 cm while the error range of the rest of the days stayed around 4 cm or less, which is the reasonable magnitude of vertical errors in kinematic PPP that are shown in many kinematic PPP studies (e.g. Anquela et al., 2012; Alkan et al., 2015; Wang et al., 2024). Horizontal

errors are generally consistent within the range of 3 cm throughout the six days. As found in Fig. 4, there were strong scintillations occurring around the end of DOY 131 that clearly affected the positioning performance where the vertical error of PPP around the end of DOY 131 reached up almost 10 cm. On DOY 132, the vertical errors remained high even though the scintillation index stayed low during that day. It can be noted that Dst values dramatically decreased at the end of DOY 131 and stayed low at the beginning of DOY 132. While the Dst values started being recovered on DOY 132, it stayed lower than –100 nT. Therefore, one can consider that there were strong geomagnetic storm effects on DOY 132 which influenced the positioning performance.

Table 2 presents the count of the kinematic PPP vertical errors in the error bins from –6 cm to +8 cm before and after the most severe storm on DOY 131-132. The data processing was conducted for a daily observation with 30 seconds of sampling interval. The reference epoch of the geomagnetic event is 20:00 UTC on DOY 131. Note that 67 data points fall into the error bins larger than ±4 cm within the 24 hours from the storm (indicated as *(+) 24 hours* in the table), that is about 2.3% of the total points, while the other two cases, within the 48 hours before the storm (indicated as *(–) 48 hours* in the table) and the 24 hours before the storm (indicated as *(–) 24 hours* in the table, have 0 and 14 data points exceed the 4 cm error which are about 0% and 0.5% of total points, respectively. This fact is considerably linked to the presence of the irregularities entering the ISMR field of view as a response to the modifications of the low-latitude electrodynamics induced by the geomagnetic superstorm. It should be noted that the receiver failed to record 35 epochs of observation within 24 hours from the storm, so that the number of total data points for the PPP solution within 24 hours from the storm is 2845, while the number of total data points of prior days, indicated as (–) 48 hours and (–) 24 hours, is 2880.

Vertical Error [cm]	(–) 48 hours	(–) 24 hours	(+) 24 hours
–6 to –4	7	0	14
–4 to –2	245	149	198
–2 to 0	1289	1171	905
0 to 2	1165	1375	1403
2 to 4	174	171	272
4 to 6	0	14	44
6 to 8	0	0	9

Table 2. Vertical error counts of PPP in the error bins of 2 cm interval –48 hours and 24 hours before the geomagnetic storm (20:00 UTC on DOY 131) representing the PPP unaffected by the storm and 24 hours after the storm indicating the effect of the storm to the PPP solutions.

To effectively evaluate the impact of the geomagnetic superstorm, we selected the five most quiet days (DOY 143, 149, 130, 125(K), 146) and the five most disturbed days (DOY 132, 131, 133, 123, 134) in May 2024, taken from the German Research Centre for Geosciences (GFZ) data center (https://kp.gfz-potsdam.de/en/data). One interesting point is that those five quietest days include DOY 130, which is the day before the sequence of strong disturbances from DOY 131 to DOY 134. In addition, the GFZ data center appended the indicator, K, to DOY 125 which indicates the high Kp values (greater than 3) even though the Ap was smaller or equal to 6. It is noteworthy that four of the five most disturbed days that are DOYs 131, 132, 133, and 134, are during the Mother's Day storm day.

To compare two extreme cases of quiet and disturbed ionospheric effect to GNSS signal processing, Fig. 6 generated by CSRS-PPP tool, presents the number of tracked satellites and the percentage of the ambiguity reset

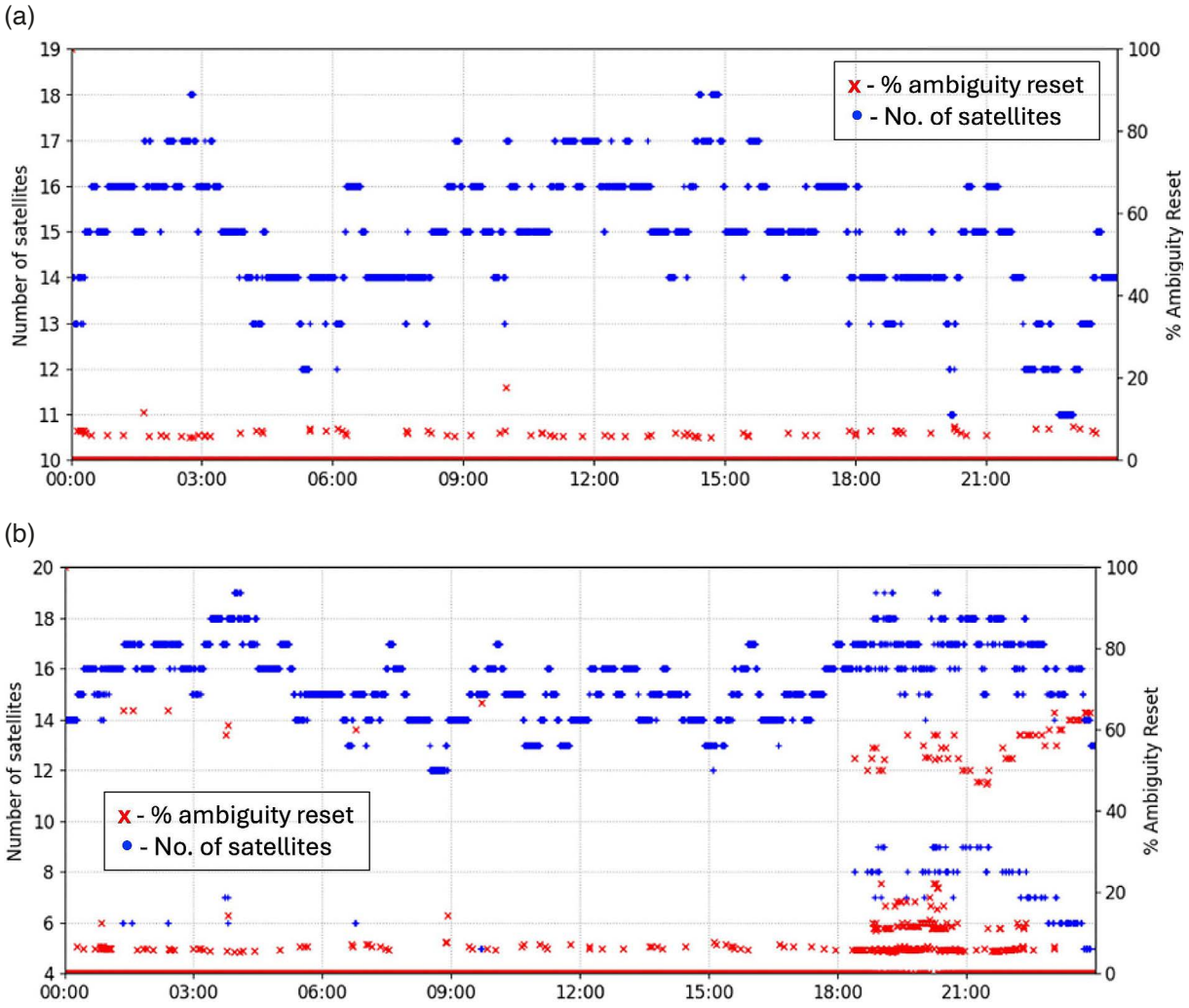

Figure 6. The number of tracked satellites (blue marks with the left axis) and the percentage of the ambiguity reset (red marks with the right axis) on DOY 149, 29 May 2024, which is one of the quietest days in May 2024 (a) and on DOY 131, which is 10 May 2024, which the most disturbed day in May 2024.

during the PPP processing on DOY 149 (28 May 2024), which is one of the quietest days in May 2024 in (a) and on DOY 131 (10 May 2024), which is the most disturbed day in May 2024 in (b).

While the number of tracked satellites was similar between the two days – except the post sunset hours on DOY 131 which dropped more satellites than DOY 149, the percentage of the ambiguity reset on the disturbed day on the bottom plot was significantly higher than the quiet day on top, especially during the later hours of the day in which the Kp indices were 8 and greater that can be found in Fig. 1. In Fig. 6b, one can see that there is a 50-60% resets in ambiguities after 18:00 UT on DOY 131.

To effectively analyze the impact of the Mother's Day storm, we evaluated the percentage of the fixed ambiguities and the positioning error per each daily processing result for the selected days that are the four quietest days (excluding DOY 143 which included the significant unknown data gaps) and four disturbed days during the Mother's day storm, which are DOYs 131, 132, 133, and 134.

Table 3 lists the percentage of fixed ambiguities in the kinematic PPP solution for the quiet and disturbed days. Clearly, the percentage of fixed ambiguities is close to or greater than 98% for the quiet days as compared to the lower than 90% on the disturbed days.

Figure 7 shows the histograms of vertical errors for the selected quiet and disturbed days in May 2024, the left and right columns, respectively. The histograms visually demonstrate that the amplitude of the vertical errors during the disturbed days is bigger than the ones on the quiet days. Tables 4 and 5 offer the numerical quantities of the vertical errors in each bin of the histograms during two different categories of ionospheric conditions.

QUIET DAYS		DISTURBED DAYS	
DOY	% Fixed Ambiguities	DOY	% Fixed Ambiguities
125	99.30	131	89.04
130	97.98	132	86.49
146	99.52	133	92.51
149	98.99	134	97.28

Table 3. Percentage of fixed ambiguities during the quiet and disturbed days.

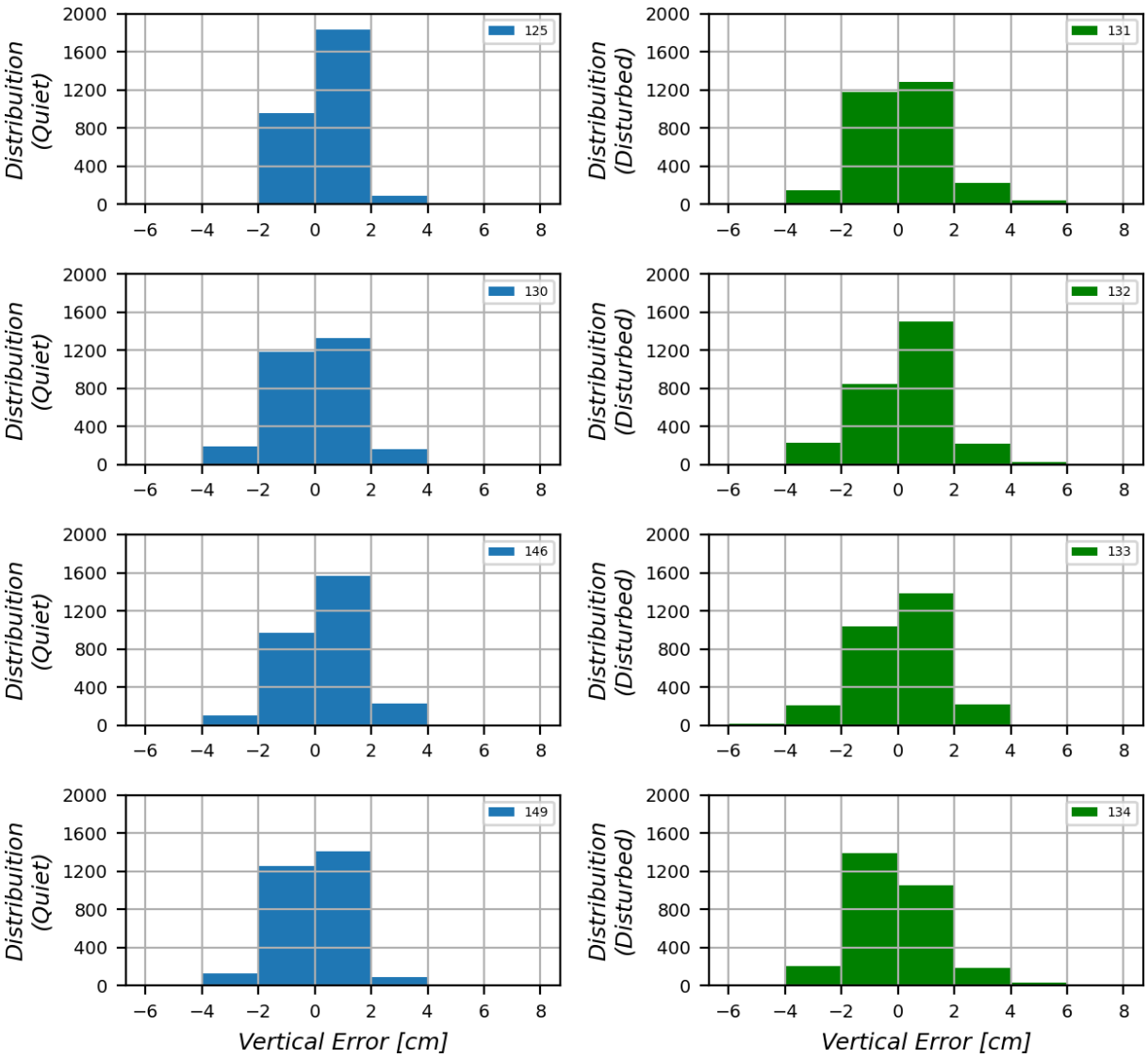

Figure 7. Histograms of the vertical error on four quiet days (blue histograms in the left column) and four most disturbed days during the Mother's Day storm (green histograms in the right column).

Vertical Error [cm]	DOY 125	DOY 130	DOY 146	DOY 149
−6 to −4	0	7	3	0
−4 to −2	9	188	99	125
−2 to 0	952	1188	974	1255
0 to 2	1828	1327	1570	1412
2 to 4	91	168	233	87
4 to 6	0	2	1	1
6 to 8	0	0	0	0
8 to 10	0	0	0	0

Table 4. Vertical error counts during the quiet days in May 2024.

Vertical Error [cm]	DOY 131	DOY 132	DOY 133	DOY 134
−6 to −4	1	13	14	4
−4 to −2	151	230	211	209
−2 to 0	1174	848	1040	1393
0 to 2	1282	1497	1384	1058
2 to 4	227	224	217	184
4 to 6	37	32	8	31
6 to 8	6	3	1	1
8 to 10	2	1	0	0

Table 5. Vertical error counts during the disturbed days in May 2024.

To quantitatively analyze the occurrence of the large errors, we computed the percentage of the errors larger than 4 cm on each day. During the quiet days, DOY 125, DOY 130, DOY 146, DOY 149, errors larger than 4 cm occurred in 0%, 0.3%, 0.1%, and 0%, respectively. It is worth noting that the positioning performance on DOY 125 was still high even though it was the recovery phase of a geomagnetic storm in early May. It was classified as a quiet day based on the Ap index only while it can be classified as a disturbed day based on the Dst and Kp values. During the disturbed days, DOY 131-DOY 134, which are the period of the Mother's Day storm, 2.9%, 1.7%, 0.8%, and 1.25% of positioning solutions showed large vertical errors, respectively. It should be noted that the receiver failed to record some epochs of observation during the three most disturbed days in May, DOY 131, 132, and 133. While the

number of data points on all quiet days and the fourth highest disturbed day, DOY 134, recorded all 2880 epochs of observation, DOY 131, 132, and 133 recorded 2878, 2847, and 2875 data points, respectively.

4. Summary and Discussion

Geomagnetic storms generate various changes and disturbances in the ionosphere, thermosphere, and magnetosphere. Many studies investigated geomagnetic storms by analyzing ionospheric observations using different sensors. As GNSS is one of the most effective sensors to observe the ionosphere, it serves as a useful tool to investigate ionospheric responses to geomagnetic storm events in terms of measuring the variation of electron content in the ionosphere and presence of small-scale irregularities causing scintillation. On the other hand, the effect of geomagnetic storms in the ionosphere causes the degradation of the GNSS positioning accuracy. While the ionospheric code delay and the phase advance can mostly be eliminated by using dual or more frequency measurements, random variations in the signal amplitude and phase due to the presence of small-scale (Fresnel's scale) irregularities raise challenges in mitigating ionospheric errors. The occurrence of such irregularities is strongly linked to the geo-space forcing due to space weather.

As mentioned in Introduction, degradation of GNSS performance caused by ionospheric irregularities can lead to severe safety issues as it is one of the most critical elements in positioning, navigation and timing (PNT). Ionospheric irregularities are mostly observed in high- and low-latitudes, while mid-latitudes are less prone to ionospheric disturbances (see e.g. Spogli et al., 2013). Irregularities at high-latitudes and related GNSS positioning errors are directly linked with the occurrence of geomagnetic storms through the magnetosphere-ionosphere coupling (see e.g. Linty et al., 2018). On the contrary, as already reported in the Introduction section, irregularity formation at low-latitudes is linked to solar flux and seasonal conditions (e.g. equinoxes are favored) influencing the formation of EPBs (Li et al., 2021; Balan et al., 2018 and references therein), in which irregularities of various scales form, and the effect of a geomagnetic storm is to inhibit or exacerbate their occurrence (Spogli et al., 2016; Alfonsi et al., 2011; 2021; Tulasi Ram et al., 2016). Very few studies focus on mid-latitude regions and, recently, the interest in such highly populated regions has started to grow rapidly.

As the Mother's Day storm is known as one of the most severe storms over the last 20 years, and obviously the biggest event in the solar cycle 25 to date, it is worth investigating its impact in different aspects. Although strong space weather events mostly affect high-latitude regions, this severe event generated visible auroras and stable auroral arcs all around the world. Consequently, this study is particularly focused on the GNSS observations at mid-latitudes to analyze and evaluate the effects in the ionosphere and GNSS positioning.

During the Mother's Day storm period, indicated by extremely high Kp indices and extremely low level of Dst, the observed TEC values in Lampedusa Island, Italy, dramatically decreased and several strong code and phase scintillations were recorded. Since the magnitude of the ionospheric error in GNSS signals is positively correlated with the TEC values, small TEC values may result in small GNSS positioning errors considering the ionospheric delay decreases. In our experiments, however, higher positioning errors occurred on DOYs 131 and 134 despite much lower TEC values on those days as shown in Fig. 3. This result can be explained by the scintillation occurrence due to the spill-over of EPBs in the field of view of the receiver and the ambiguity reset rates that are shown from Fig. 4 through Fig. 6. Although the negative storm over Italy led to a decrease in the TEC values, the strong disturbances occurred, and they directly affected the GNSS signal tracking capability resulting in frequent ambiguity resets during those days.

Another point of discussion is the notable degradation of GNSS positioning at the mid-latitude area that has not been commonly shown in the past. Considering the importance of the GNSS in PNT, proper strategies for mitigating the effect are necessary for public safety. While several studies (e.g. Aquino et al., 2009; Park et al., 2017) demonstrated methods to mitigate the scintillation effects for high-accuracy solutions, few studies investigated the mitigation approach for mid-latitudes.

Our findings highlight that the spill-over of EPBs into mid-latitudes represents a critical aspect of ionospheric behavior during geomagnetic storms, challenging conventional assumptions that such disturbances are confined to equatorial or polar regions. This novel perspective is pivotal for refining GNSS models and developing robust mitigation strategies, especially for regions previously considered immune to severe ionospheric impacts. ng. For further research, comprehensive analysis in diverse stations over the world during different levels and different longitudinal development of geomagnetic storms will be done that can offer a better understanding of the space weather events and their effect on GNSS PNT.

5. Conclusions

The Mother's Day geomagnetic storm in May 2024 had a profound impact on ionospheric conditions at mid-latitudes, an area typically considered less affected by such events. Observations from Lampedusa, Italy, revealed a significant TEC depletion, classifying the event as a "negative storm." Additionally, strong amplitude scintillations and phase fluctuations were recorded, particularly shortly after the storm onset, which directly degraded the quality of GNSS signals. GNSS positioning errors during the storm period increased significantly. On the disturbed days, the 1-2% of the kinematic PPP solutions fell into the range of the vertical error above 4 cm and while less than 0.4% of positioning results exceeded 4 cm error on the quiet days.

The storm also caused frequent ambiguity resets in GNSS processing, particularly on the most disturbed days, emphasizing the vulnerability of GNSS systems at mid-latitudes during extreme space weather events. These findings challenge the common perception that mid-latitudes are not susceptible to ionospheric disturbances compared to high- or low-latitude regions. This underscores the critical need for robust mitigation strategies to safeguard PNT applications, particularly in scenarios where safety is paramount.

This study is contributing to shed light on the behavior of ionospheric disturbances at mid-latitudes, particularly in relation to extreme space weather events. By documenting the spill-over effects of EPBs during the strongest geomagnetic storm of solar cycle 25 and assessing the impact on precise point positioning, our findings emphasize the necessity to broaden the scope of GNSS vulnerability assessments to include regions traditionally deemed stable.

The study emphasizes the importance of further research to analyze GNSS data across diverse global regions and varying levels of geomagnetic storm intensity. This broader investigation would enhance understanding of the impacts of space weather on GNSS and support the development of effective mitigation strategies.

Acknowledgements. We acknowledge Dr. Emanuele Pica from INGV for his contributions by creating Fig. 1 and providing GNSS files for the data processing and analysis in this study.

References

Alfonsi, L., L. Spogli, J. R. Tong, G. De Franceschi et al. (2011). GPS scintillation and TEC gradients at equatorial latitudes in April 2006, Adv. Space Res., 47, 10, 1750-1757, doi:10.1016/j.asr.2010.04.020.

Alfonsi, L., C. Cesaroni, L. Spogli, M. Regi et al. (2021). Ionospheric disturbances over the Indian sector during 8 September 2017 geomagnetic storm: Plasma structuring and propagation, Space Weather, 19, 3, e2020SW002607, doi:10.1029/2020SW002607.

Alkan, R. M., V. İlçi, I. M. Ozulu and M. H. Saka (2015). A comparative study for accuracy assessment of PPP technique using GPS and GLONASS in urban areas, Measurement, 69, doi:10.1016/j.measurement.2015.03.012.

Anguela, A. B., A. Martin, J. L. Berné and J. Padin (2012). GPS and GLONASS Static and Kinematic PPP results, J. Surv. Eng., 139, 1, doi:10.1061/(ASCE)SU.1943-5428.0000091.

Aquino, M., J. F. G. Monico, A. H. Dodson, H. Marques et al. (2009). Improving the GNSS Positioning Stochastic Model in the Presence of Ionospheric Scintillation, J. Geod., 83, 10, 953-966, doi:10.1007/s00190-009-0313-6.

Balan, N., L. Liu and H. Le (2018). A brief review of equatorial ionization anomaly and ionospheric irregularities, Earth Planet. Phys., 2, 4, 257-275, doi:10.26464/epp2018025.

Basu, S., J. J. Makela, E. MacKenzie, P. Doherty et al. (2008). Large magnetic storm-induced nighttime ionospheric flows at midlatitudes and their impacts on GPS-based navigation systems, J. Geophys. Res. Space, 113, A00A06, doi:10.1029/2008JA013076, 2008.

Bougard, B., J. M. Sleewaegen, L. Spogli, S. V. Veettil et al. (2011). CIGALA: Challenging the solar maximum in Brazil with PolaRxS, in Proceedings of the 24th International Technical Meeting of the Satellite Division of the Institute of Navigation, ION GNSS 2011, Portland, OR, 2572-2579.

Cesaroni, C., L. Spogli and G. De Franceschi (2021). IONORING: Real-time monitoring of the total electron content over Italy, Remote Sens., 13, 16, 3290, doi:10.3390/rs13163290.

Cesaroni, C., L. Alfonsi, M. Pezzopane, C. Martinis et al. (2017). The first use of coordinated ionospheric radio and optical observations over Italy: Convergence of high-and low-latitude storm-induced effects, J. Geophys. Res. Space Phys., 122, 11, 11-794, doi:10.1002/2017JA024325.

Ciraolo, L., F. Azpilicueta, C. Brunini, A. Meza et al. (2007). Calibration errors on experimental slant total electron content (TEC) determined with GPS, J. Geod., 81, 2, 111-120, doi:10.1007/s00190-006-0093-1.

Evans, J. S., J. Correira, J. D. Lumpe, R. W. Eastes et al. (2024). GOLD observations of the thermospheric response to the 10-12 May 2024 Gannon superstorm, Geophys. Res. Lett., 51, e2024GL110506, doi:10.1029/2024GL110506.

Guo, X., B. Zhao, T. Yu, H. Hao et al. (2024). East-west difference in the ionospheric response during the recovery phase of May 2024 super geomagnetic storm over the East Asian, J. Geophys. Res. Space Phys., 129, e2024JA033170, doi:10.1029/2024JA033170.

Kashcheyev, A., Y. Migoya-Orué, C. Amory-Mazaudier, R. Fleury et al. (2018). Multivariable comprehensive analysis of two great geomagnetic storms of 2015, J. Geophys. Res. Space Phys., 123, 5000-5018, doi:10.1029/2017JA024900.

Kauristie, K., J. Andries, P. Beck, J. Berdermann et al. (2021). Space weather services for civil aviation – Challenges and solutions, Remote Sens., 13, 18, 3685, doi:10.3390/rs13183685.

Li, G., B. Ning, Y. Otsuka, M. A. Abdu et al. (2021). Challenges to equatorial plasma bubble and ionospheric scintillation short-term forecasting and future aspects in east and southeast Asia, Surv. Geophys., 42, 201-238, doi:10.1007/s10712-020-09613-5.

Linty, N., A. Minetto, F. Dovis and L. Spogli (2018). Effects of phase scintillation on the GNSS positioning error during the September 2017 storm at Svalbard, Space Weather, 16, 9, 1317-1329, doi:10.1029/2018SW001940.

Luo, X., S. Gu, Y. Lou, C. Xiong et al. (2018). Assessing the Performance of GPS Precise Point Positioning Under Different Geomagnetic Storm Conditions during Solar Cycle 24, Sensors, 18, 1784, doi:10.3390/s18061784.

Macho, E. P., E. Correia, L. Spogli and M. T. Muella (2022). Climatology of ionospheric amplitude scintillation on GNSS signals at south American sector during solar cycle 24, J. Atmos. Sol. Terr. Phys., 231, 105872, doi:10.1016/j.jastp.2022.105872.

Mendillo, M. (2006). Storms in the ionosphere: Patterns and processes for total electron content, Rev. Geophys., 44, 4, doi:10.1029/2005RG000193.

Mrak, S., A. J. Coster, K. Groves and R. Nikoukar (2023). Ground-based infrastructure for monitoring and characterizing intermediate-scale ionospheric irregularities at mid-latitudes, Front. Astron. Space Sci., 10, 1091340, doi:10.3389/fspas.2023.1091340.

Nava, B., J. Rodríguez-Zuluaga, K. Alazo-Cuartas, A. Kashcheyev et al. (2016). Middle and low latitude ionosphere response to 2015 St. Patrick's Day geomagnetic storm, J. Geophys. Res. Space Phys., 2016, doi:10.1002/2015JA022299.

NOAA Space Weather Scales (2025). NOAA Space Weather Scales | NOAA / NWS Space Weather Prediction Center (n.d.), https://www.swpc.noaa.gov/noaa-scales-explanation.

Park, J., S. Veettil, M. Aquino, L. Yang et al. (2017). Mitigation of Ionospheric Effects on GNSS Positioning at Low Latitudes, Navig. J. Inst. Navig., 64, 1, doi:10.1002/navi.177.

Pica, E., A. Minetto, C. Cesaroni and F. Dovis (2023). Analysis and Characterization of an Unclassified RFI Affecting Ionospheric Amplitude Scintillation Index over the Mediterranean Area, IEEE J. Sel. Top. Appl. Earth Obs. Remote Sens., 99, 1-20, doi:10.1109/JSTARS.2023.3267003.

Pica, E., L. Spogli, C. Cesaroni, L. Alfonsi et al. (2024). Assessing the ionospheric scintillations occurrence on L-band in the southern Mediterranean sector, Authorea Preprints, doi:10.22541/essoar.172222578.89374019/v1.

Pignalberi, A., C. Cesaroni, M. Pietrella, M. Pezzopane et al. (2024). Ionospheric nowcasting over Italy through data assimilation: A synergy between IRI UP and IONORING, Space Weather, 22, 5, e2023SW003838, doi:10.1029/2023SW003838.

Rodrigues, F. S., J. G. Socola, A. O. Moraes, C. Martinis et al. (2021). On the properties of and ionospheric conditions associated with a mid-latitude scintillation event observed over southern United States, Space Weather, 19, 6, e2021SW002744, doi:10.1029/2021SW002744.

Shinbori, A., Y. Otsuka, T. Tsugawa, M. Nishioka et al. (2021). Relationship between the locations of the midlatitude trough and plasmapause using GNSS TEC and Arase satellite observation data, J. Geophys. Res. Space Phys., 126, 5, e28943, doi:10.1029/2020JA028943.

Spogli, L., L. Alfonsi, P. J. Cilliers, E. Correia et al. (2013). GPS scintillations and total electron content climatology in the southern low, middle and high latitude regions, Ann. Geophys., 56, 2, R0220, doi:10.4401/ag-6240.

Spogli, L., C. Cesaroni, D. Di Mauro, M. Pezzopane et al. (2016). Formation of ionospheric irregularities over Southeast Asia during the 2015 St. Patrick's Day storm, J. Geophys. Res. Space Phys., 121, 12, 12-211, doi:10.1002/2016JA023222.

Spogli, L., D. Sabbagh, M. Regi, C. Cesaroni et al. (2021). Ionospheric response over Brazil to the August 2018 geomagnetic storm as probed by CSES-01 and Swarm satellites and by local ground-based observations, J. Geophys. Res. Space Phys., 126, 2, e2020JA028368, doi:10.1029/2020JA028368.

Spogli, L., L. Alfonsi and C. Cesaroni (2023). Stepping into an equatorial plasma bubble with a Swarm overfly, Space Weather, 21, 5, e2022SW003331, doi:10.1029/2022SW003331.

Spogli, L., T. Alberti, P. Bagiacchi, L. Cafarella et al. (2024). The effects of the May 2024 Mother's Day superstorm over the Mediterranean sector: from data to public communication, Ann. Geophys., 67, 2, PA218, doi:10.4401/ag-9117.

Themens, D. R., S. Elvidge, A. McCaffrey, P. T. Jayachandran et al. (2024), The High Latitude Ionospheric Response to the Major May 2024 Geomagnetic Storm: A Synoptic View, Geophys. Res. Lett., doi:10.1029/2024GL111677.

Tornatore, V., C. Cesaroni, M. Pezzopane, M. M. Alizadeh et al. (2021). Performance evaluation of VTEC GIMs for regional applications during different solar activity periods, using RING TEC values, Remote Sens., 13, 8, 1470, doi:10.3390/rs13081470.

Tulasi Ram, S., T. Yokoyama, Y. Otsuka, K. Shiokawa et al. (2016). Duskside enhancement of equatorial zonal electric field response to convection electric fields during the St. Patrick's Day storm on 17 March 2015, J. Geophys. Res. Space Phys., 121, 1, 538-548, doi:10.1002/2015JA021932.

Vadakke Veettil, S. and M. Aquino (2021). Statistical models to provide meaningful information to GNSS users in the presence of ionospheric scintillation, GPS Solut., 25, 2, 54, doi:10.1007/s10291-020-01083-x.

Wernik, A. W., J. A. Secan and E. J. Fremouw (2003). Ionospheric irregularities and scintillation, Adv. Space Res., 31, 4, 971-981, doi:10.1016/S0273-1177(02)00795-0.

Wang, S., R. Tu, J. Hong and X. Lu (2024). A novel stop-and-go kinematic positioning method for PPP-RTK, A novel stop-and-go kinematic positioning method for PPP-RTK, Geo-Spat. Inf. Sci., 1-14, doi:10.1080/10095020.2024.2338227.

Yamazaki, Y. and A. Maute (2017). Sq and EEJ – A review on the daily variation of the geomagnetic field caused by ionospheric dynamo currents, Space Sci. Rev., 206, 1, 299-405, doi:10.1007/s11214-016-0282-z.

Yeh, K. C. and C. H. Liu (1982). Radio wave scintillations in the ionosphere, Proceedings of the IEEE, 70, 4, 324-360, doi:10.1109/PROC.1982.12313.

Yizengaw, E. and K. M. Groves (2018). Longitudinal and seasonal variability of equatorial ionospheric irregularities and electrodynamics, Space Weather, 16, 8, 946-968, doi:10.1029/2018SW001980.

***CORRESPONDING AUTHOR: Jihye PARK**,
Oregon State University, School of Civil and Construction Engineering, Corvallis, Oregon, USA
e-mail: Jihye.Park@oregonstate.edu